SEMI-RIGID STRUCTURES FOR SPACE APPLICATIONS

EXPANDABLE SPACE STRUCTURE

P. M. Knox, Jr.
R. O. Moses

MARTIN COMPANY

INTRODUCTION

This development program was initiated by the Manufacturing Technology Division of the Air Force Materials Laboratory and the Air Force Flight Dynamics Laboratory, Wright-Patterson Air Force Base, to determine and develop the manufacturing methods, processes, and related design data required for the efficient and practical use of available materials for expandable space structures under Contract AF 33(657)-9733.

Future operational mission requirements for space vehicles or stations will necessitate a substantial increase in payload size and weight, and therefore increased booster requirements. Alleviation of these booster requirements can be aided by the design of efficient space structures. One such structural concept is the expandable semirigid or telescoping structure. The effort covered by this contract is to develop the manufacturing knowhow for a telescoping space structure and establish its feasibility by evaluation and test for use as a manned space station.

The predominating considerations for the conventional space structure are:

1) Sealing and control of air leakage due to meteoroid penetration;

2) Environmental control;

3) Systems integration;

4) Compatibility of materials with natural and induced environments;

5) Structural and mechanical considerations.

The concept of Expandable Space Structures (ESS) introduces several new problems:

1) Structural integrity of telescoping structures;

2) Mechanical feasibility of stowage and deployment in a space environment;

3) Tooling and manufacturing problems associated with stowage and deployment requirements.

Design, fabrication, and ground testing of a semirigid telescoping expandable space structure (ESS) is covered in this paper. The work was performed in three phases: Phase I, design; Phase II, manufacturing; and Phase III, testing.

VEHICLE CONCEPT

The expandable space structure (ESS) program is oriented around a telescoping semirigid structure concept. This concept provides a collapsible structure for minimum size when required, and yet provides a rigid, metallic, large-volume structure after expansion to full length. The structural concept can be used for a complete space vehicle structure or for portions of the complete structure. An expandable space structure provides a low-length, reduced-volume payload to minimize boost phase flight problems and permit maximum use of the payload booster capability. Once in orbit it may be expanded to produce a useful volume for astronaut occupancy, equipment relocation, or numerous other applications discussed below.

The design concept provides a leak tight vehicle capable of maintaining an atmosphere for its occupants. It is of double-wall construction for maximum protection against meteoroids, and can maintain a livable temperature environment by passive thermal control using paint coatings or by an active radiator system. An R&D structure designed around this concept is seen in Fig. 1. This design may be varied in size, number of telescoping segments, and in various details for different applications.

DESIGN CRITERIA

The basic philosophy governing vehicle design is to develop an expanding structure that will prove concept feasibility. Design of the expandable sections considered the requirements of a manned space station. Portions of the vehicle not pertinent to proving concept feasibility, such as end closures, are designed for proper functioning of the telescoping structure, but need not be of the configuration proposed for space flight.

1. Functional Requirements

The following requirements were considered in vehicle design:

a. Performance in low-earth orbits (maximum 500 mi.);

b. Maintain internal pressurization of 7 to 15 psi and loads resulting from same;

c. Radiation shielding of occupants and equipment (5 to 30 days);

d. Structural life expectancy of 1 year;

e. Minimum weight construction;

f. Material shielding and self-sealing characteristics;

g. Thermal control - external surface temperature of -150 to 400°F;

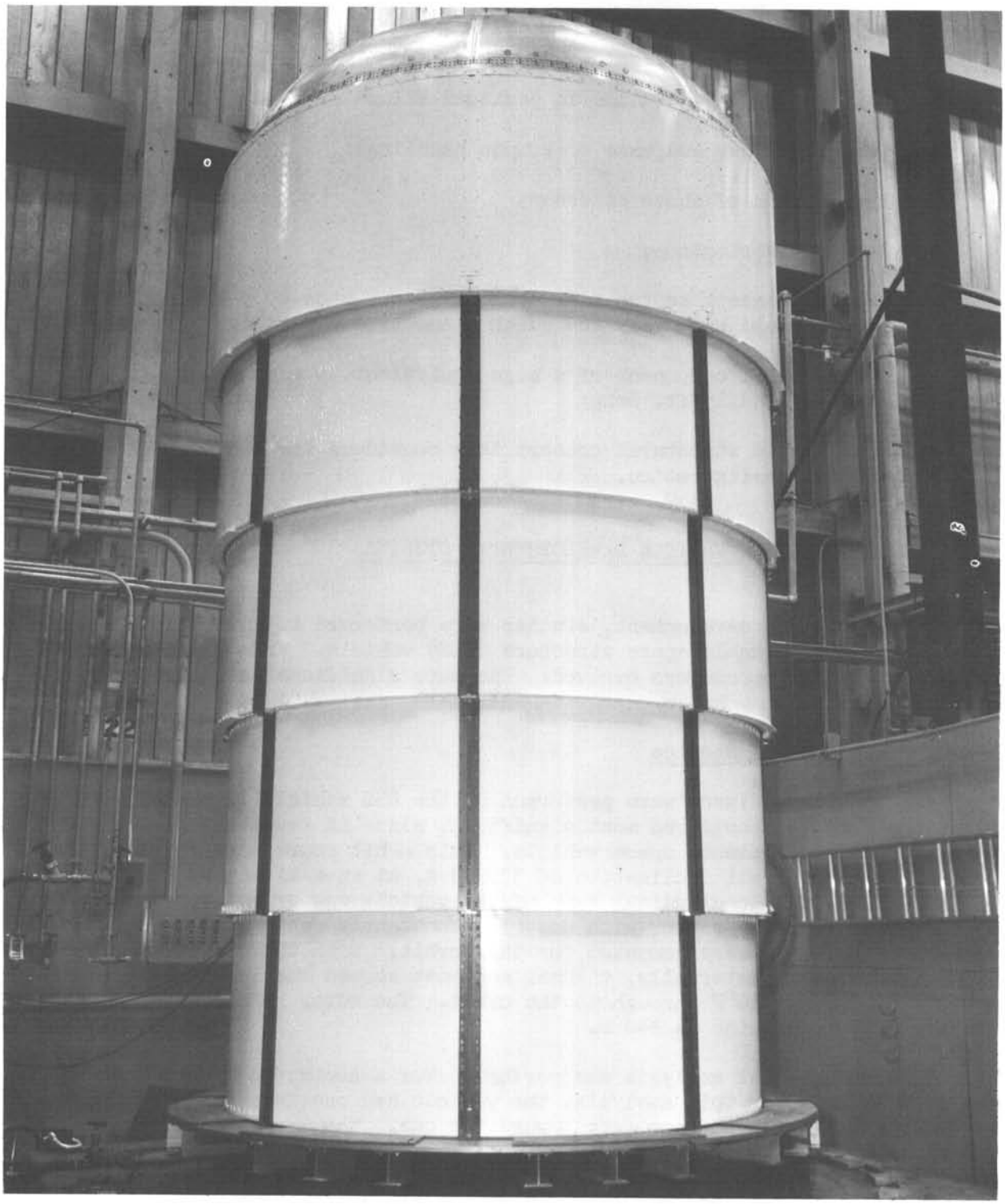

Fig. 1 ESS Vehicle Fully Extended

h. Methods and reliability of deployment;

i. Vibration and dynamic loading during launch and boost trajectory;

j. Loads imposed on structure during deployment;

k. Ratio of deployed volume to packaged volume of 5 to 1 or more;

l. Packageability and ease of ground handling;

m. Interaction of above stresses;

n. Ease of fabrication;

o. Modular concept so two similar modules, if made to rendezvous in space, would have easy and quick connection capability to each other;

p. A structural component of a size equivalent to a cylinder 8 ft. in diameter and 15 ft. long;

q. A semirigid structural concept that considers the telescoping rigid section configuration.

VEHICLE DEVELOPMENTAL STUDIES

During vehicle development, studies were performed to assist in the actual design of the expandable space structure (ESS) vehicle. From these, some of the actual design parameters evolved. The more significant studies performed are listed below.

1. Thermal Control Studies

Two thermal analyses were performed of the ESS vehicle in orbit. The first analysis is considered most significant since it investigates a more likely orbit for a manned space vehicle. This orbit represents an east launch from AMR into an orbit inclination of 33.3 deg, at an altitude of 257 n.mi. In this orbit, the longitudinal axis of the vehicle was oriented perpendicular to the orbit velocity vector with one side constantly facing the earth. Vehicle temperatures were computed for this orbit. With the air temperature maintained at 70°F internally, thermal analyses showed the inner skin temperature stayed 50° ± 10°F throughout the orbit. The outer skins varied from as low as -80°F to as high as +40°F.

A second thermal analysis was performed for a northward launch into a twilight orbit. For this analysis, the vehicle had one face oriented constantly toward the earth and another face toward the sun. The longitudinal axis of the vehicle was parallel to the orbital velocity vector. There is no roll about the longitudinal axis. Thermally, this orbit condition is more severe than that described first, and represents a steady-state heat flux condition to the vehicle. This orbit was chosen for environmental chamber testing of the vehicle

because of its test simplicity. Steady-state heat fluxes can be simulated in the chamber rather than transient rotating fluxes. Vehicle skin temperatures were computed for this orbit condition with the internal air temperature again maintained at 70°F. The inner skin temperatures varied from +62°F on the hottest side to +33°F on the coldest side. The external skin temperature varied from +38°F on the hottest side to -80°F on the coldest side.

2. Space Radiation Studies

The aluminum structure of the ESS vehicle has a unit shielding weight of 0.411 gm/cm^2. The rubberized fabric bladder in the vehicle has a unit weight of 0.071 gm/cm^2 and is equivalent to at least that much aluminum, giving a total effect shielding weight of 0.482 gm/cm^2. The total dose rates were computed, assuming the permissible dose to the crew to be 50 rad. The results are shown in Fig. 2. The orbit inclination chosen for the ESS vehicle proved to be a poor choice from a radiation dosage standpoint and would permit less than two days in orbit for the maximum permissible dosage to the crew. Orbital inclinations of less than 10 deg, however, would permit flight durations longer than a year for the selected altitude and maximum dosage. The rubber bladder should be good for about 40 years assuming a damage threshold of 10^6 rad. The aluminum structure would be sound for at least 10^{10} years.

3. Puncture Pressure Loss

Analyses were performed of vehicle leakdown rates to determine how much time an astronaut would have to find a puncture leak and repair it. Fig. 3 shows the results of this analysis. For an extremely small hole of 0.003-in. diameter, which would be very difficult to find, it would take approximately 90 days for the pressure to leak down from 11 psi to 8 psi. For a considerably larger hole of 0.10-in. diameter, that can probably be found by sound, approximately two hours are required for the same pressure decay. The study has shown that an astronaut should have adequate time to find and plug a leak before the cabin pressure leaks down to a dangerous level.

VEHICLE DEVELOPMENT TESTS

Developmental tests were performed in support of the expandable space structure (ESS) program for design areas that were in doubt, or where data were not available.

1. Panel Sealing Tests

In the interest of program economy the ESS vehicle was designed of conventional riveted structure rather than welded structure. Welded structure would provide a lower leak rate than riveted structure, but it was thought that the difference in leakage rates would be negligible. Welding the structure would result in structural distortions detrimental to demonstration of the telescoping principle, and would require development of special costly welding fixtures. Test panels of typical joints and splices were tested to determine

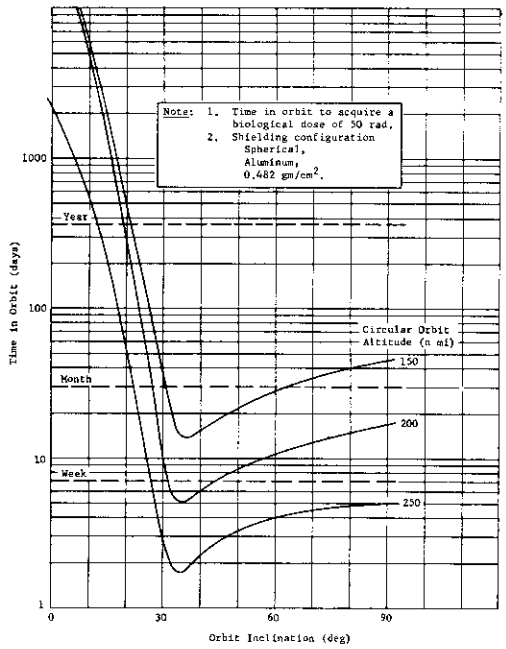

Fig. 2 Nuclear Radiation Biological Limits

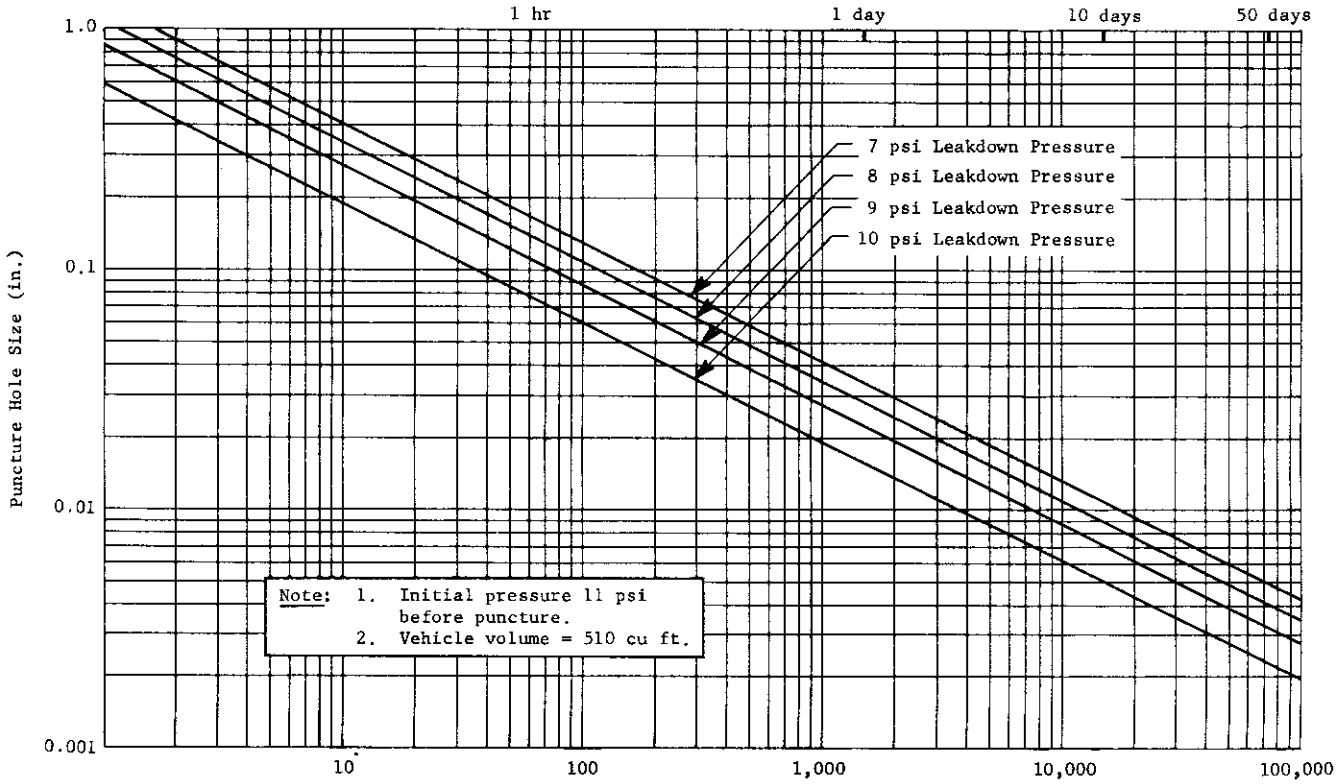

Fig. 3 Time in Minutes to Leak Down to Pressure

the adequacy of the seal-riveted structure. The panels simulated the joint used in vehicle fabrication and the kind of sealing used for that joint. The panels were mounted in a pressure vessel and leak-tested by applying a differential pressure across them. The pressure vessel test fixture is seen in Fig. 4. A typical sealant test panel is shown in Fig. 5. Only one panel indicated a leak, and this leak was attributed to the test setup rather than the panel.

2. Meteoroid Penetration Tests

A survey of meteoroid testing data was performed in support of the Expandable Space Structure Program. In addition, meteoroid penetration testing of the structure was performed by Martin using the two-stage light-gas gun facility at Denver Research Institute.

The Martin generated single-wall data reflect the testing technique of firing as many as five different sizes of glass balls at a shot. By this means, several brackets on critical ball size at a velocity near 17,000 ft/sec were obtained. Because of occasional breakup of a glass ball, some shots produced only one end of a bracket. On two occasions, a produced puncture was marginal, and it could be plotted as a point. The highest single-wall data point was obtained from a 3-mm ball at 24,000 fps. A typical test panel is shown in Fig. 7. Puncture data from single-wall penetrations are shown in Fig. 6.

The double-wall shots were fired using groups of three glass balls of nearly identical size, at velocities from 17,000 to 24,000 fps. At the higher velocities, it was found that so little separation between balls and sabot occurred, and so many balls broke up, that this multiple bead technique was necessary to produce identifiable data. Thus, each shot could give only one end of a bracket, and many produced no usable data.

The open points in Fig. 6 indicate double-wall targets with 0.020 2024 T3 bumpers spaced 1.0 in. away from 2024 T3 walls. Arrows indicate the directions of the brackets bounded by each data point. Solid points indicate targets identical to the open ones, except that the space between bumper and wall was filled with 3-pcf polyurethane foam.

Although data are inconclusive so far, it appears that on a weight basis (Fig. 6) the foam does not produce the large increase in stopping efficiency that was anticipated. The foam appears to channel the fragments of a shattered bead rather than to increase their spread, although absorbing much of their energy. Bead penetrations, with and without foam, were very similar, characterized by a thin spall off the back of the inner wall.

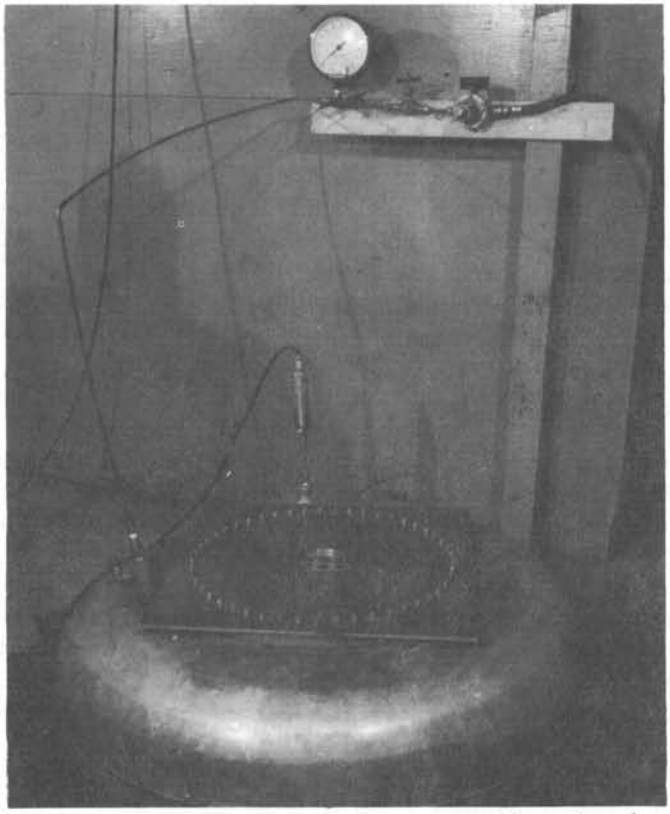

Fig. 4 Pressure Test Fixture for Panel Sealing Leak Test

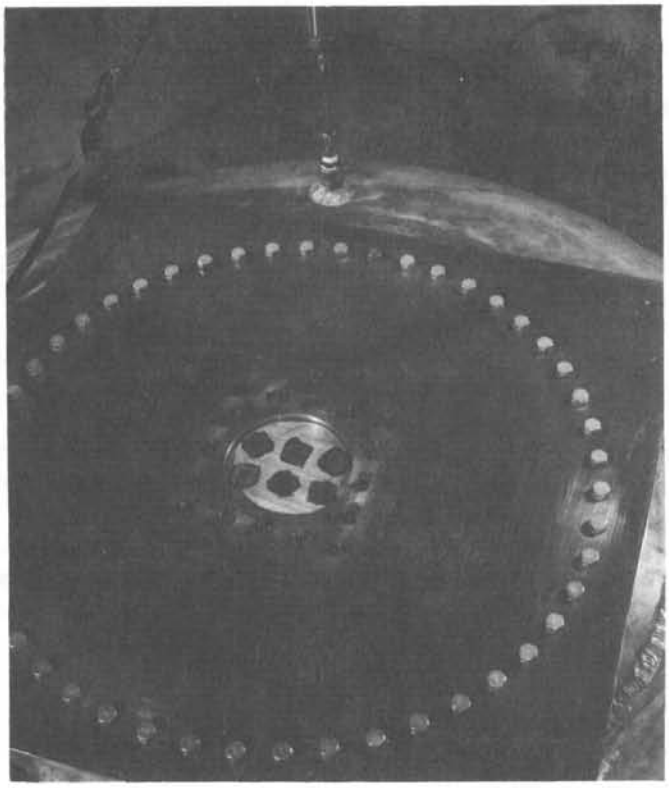

Fig. 5 Typical Test Panel

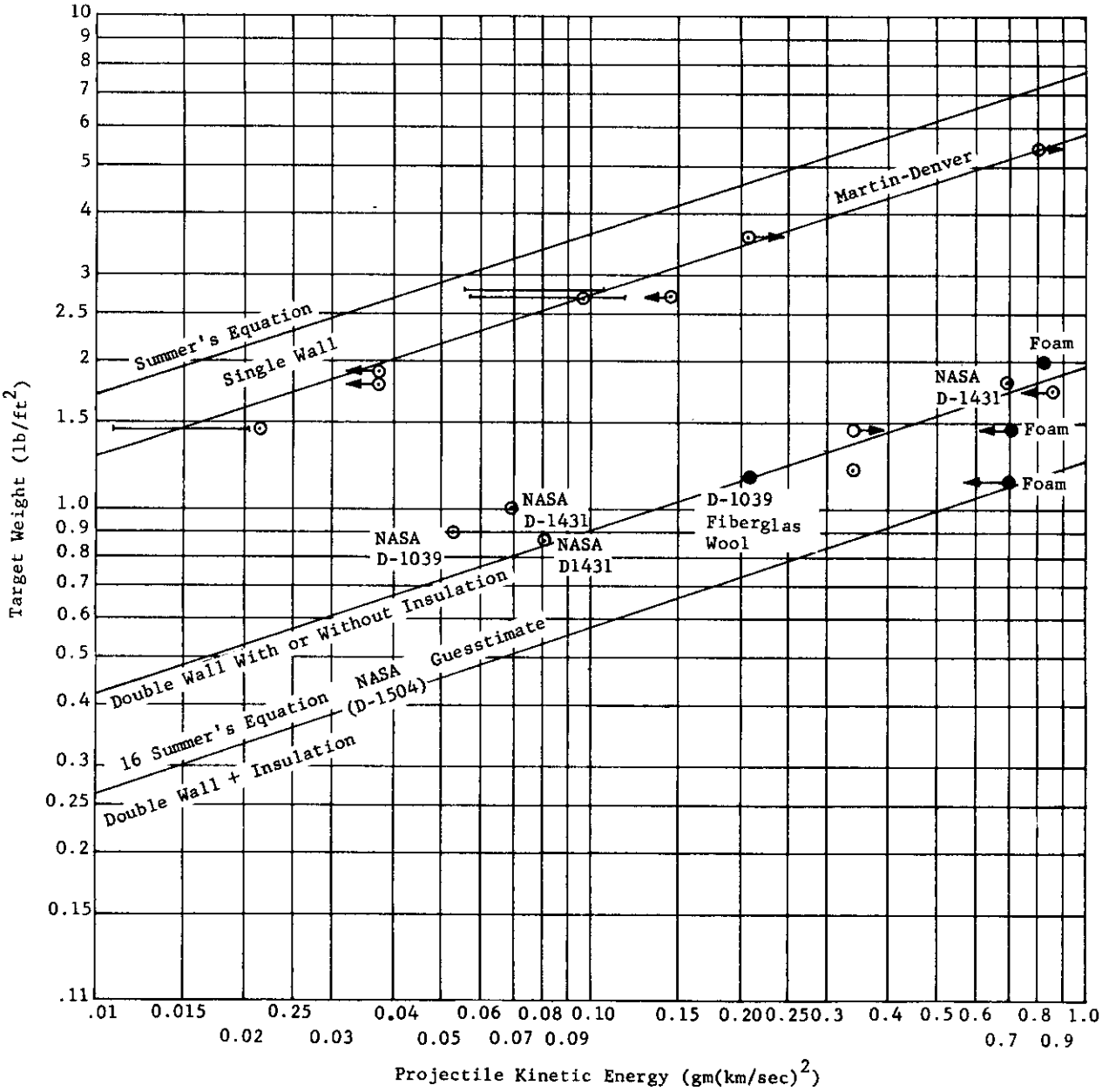

Fig. 6 Penetration Correlations, Glass Balls, Aluminum Targets

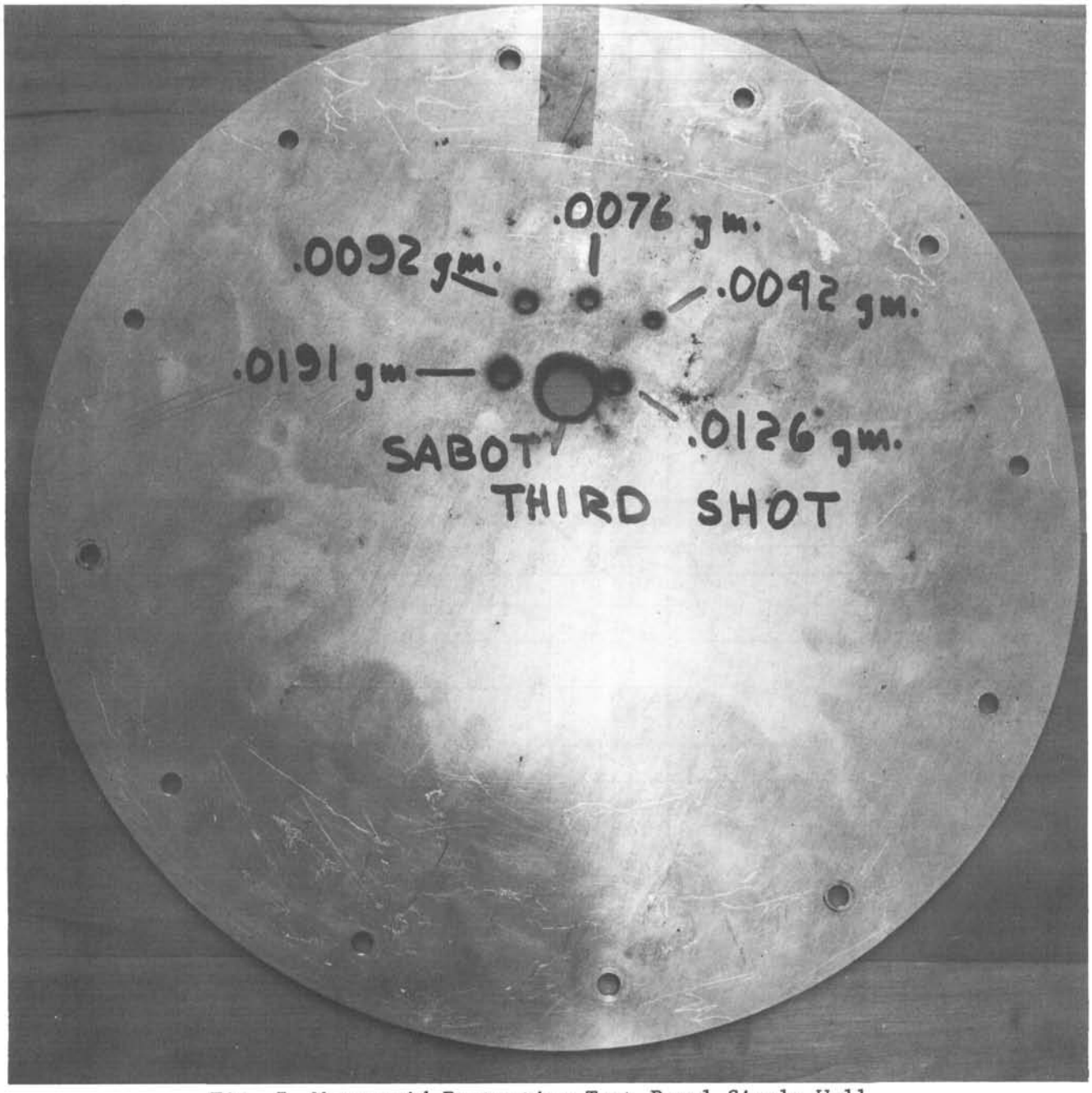

Fig. 7 Meteoroid Protection Test Panel Single Wall

3. Hypervelocity Penetration Stressed-Panel Test

Hypervelocity penetration tests of stressed panels were performed at puncture velocities slightly supersonic in the test panel material. For these tests glass beads were fired at the targets in the velocity range of 17,500 to 18,000 fps. The speed of sound in aluminum is approximately 16,740 fps.

A special pressure vessel test fixture (Fig. 8) was designed for the hypervelocity gun target chamber. This fixture provided a pressure differential across the test panel to achieve the desired stress level. An aluminum meteoroid bumper sheet was placed about 1-in. in front of the panel to simulate double-wall structure. Figure 9 shows a panel that ruptured at a stress of 28,000 psi.

Only five shots were fired in this test series. The tests were started at a stress level of 43,000 psi (yield stress) and carried downward to 28,000 psi. Since the results were somewhat erratic, much more testing is needed to pin down accurate stress levels of catastrophic rupture. However, it appears that large diameter punctures, say 1-in. diameter, will produce catastrophic rupture below 28,000 psi.

VEHICLE DESIGN

A prototype expandable space structure (ESS) design meeting design criteria requirements and incorporating design features resulting from developmental studies and tests is shown in Fig. 1. Major dimensions are given in Fig. 10. The vehicle design represents an 8-ft. diameter vehicle, 15-ft. long in the extended configuration and 5½-ft. long in the retracted configuration. The telescoping portion that demonstrates the expandable principal has five sections, is 32-in. long in the retracted configuration and slightly over 12-ft. long when extended. It has a ratio of expanded to retracted internal volume of 5.45.

A. Structural Configuration

Each telescoping section is identical in construction to other sections with the exception of top and bottom end closure provisions. Each section consists of a double-wall, sheet metal barrel with machined ring frames at each end for structural load transfer from one section to the next. Longitudinal "hat-section" stringers provide for separation of inner structural and outer meteoroid skins. The structural configuration is shown in Fig. 11. Riveted construction is used for joining all sheet metal and for joining inner structural skins to the end frames. The structural components are discussed below.

1. Machined End Frames

The end frames are designed from 7079-T652 rolled-ring forgings. This is a heat-treated and compression-stress-relieved material possessing excellent strength properties, and is dimensionally stable for machining. The cross

Fig. 8 Pressure Test Fixture for Hypervelocity Meteoroid Penetration of Stressed Panels

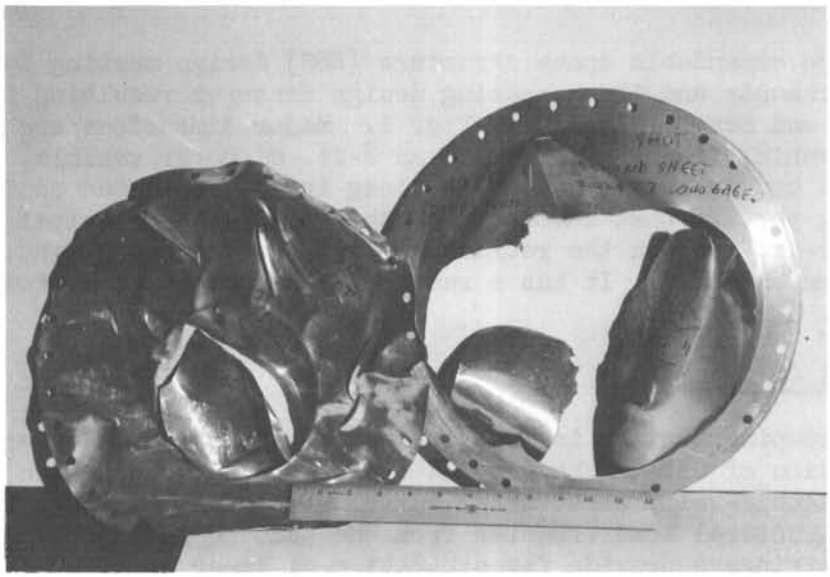

Fig. 9 Ruptured Panel Hypervelocity Penetration Test

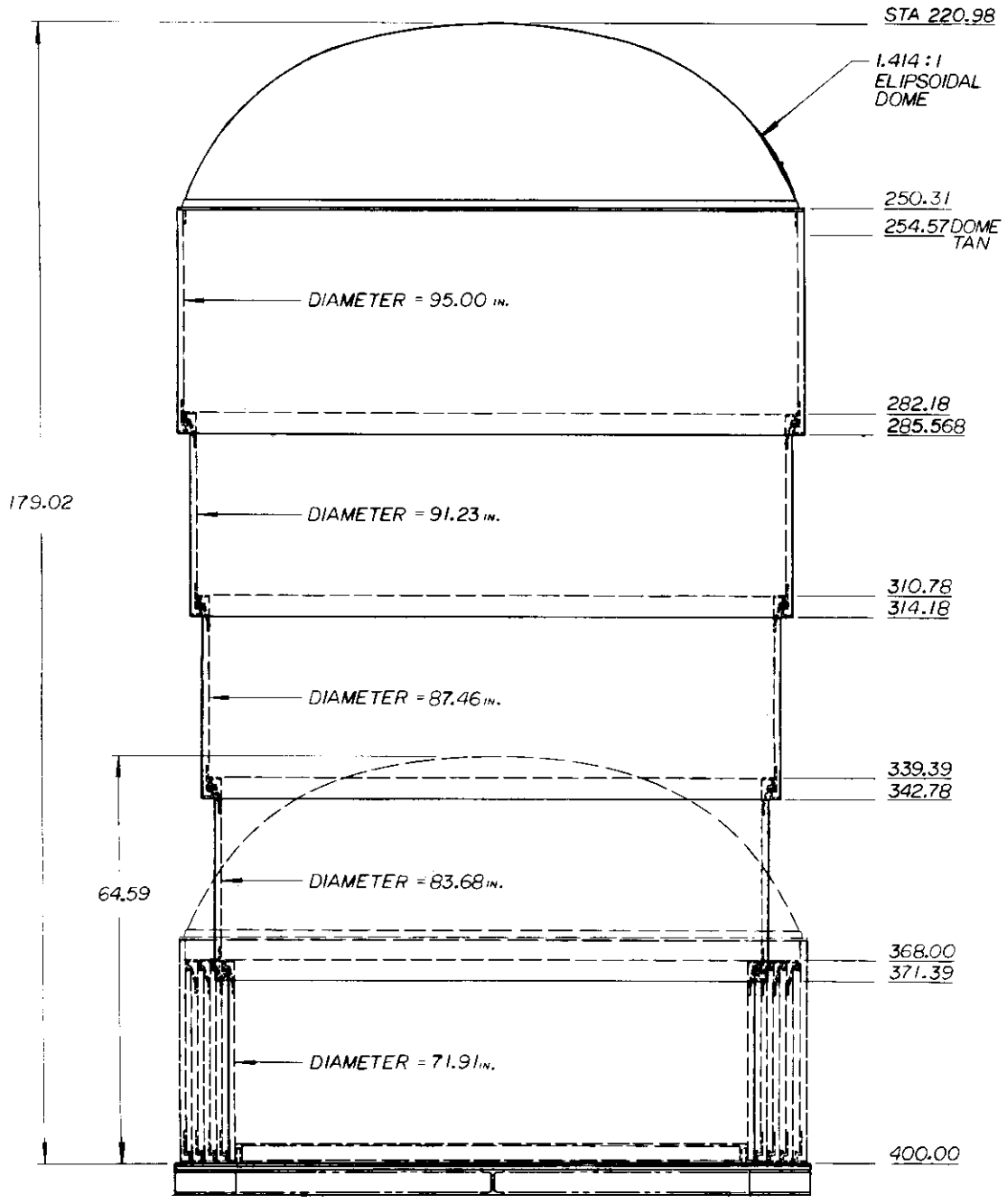

Fig. 10 Longitudinal Section of Vehicle

section of a pair of mating frames is shown in Fig. 12, depicting the forward frame of one telescoping section mated with the aft frame of the adjacent section.

In all cases the inner skin is the structural skin. Local moments produced by axial pressure loads are reacted within the frames themselves.

2. Floating Skins

To prevent severe thermal stresses within the vehicle structure the outer skins are free floating with respect to the inner skins. Analyses show that considerably greater thermal fluctuations occur in the outer skins than in the inner skins in a space environment. The free-floating characteristics permit the outer skin to expand or contract without loading the sub-structure. The free-floating feature is accomplished by oversize holes in the outer skins.

3. Forward Closure

For program economy, the forward closure of the vehicle uses a surplus Titan I dome. The attachment frame which joins the dome to the vehicle was designed of 7079-T652 aluminum alloy.

The aft bulkhead, a noncritical item for feasibility demonstration of the telescoping system, is a structural component with strength capability and reliability greater than that of the telescoping portion of the vehicle. Consequently, a machined-from-plate waffle bulkhead was designed for this application weighing about 100 pounds more than the honeycomb bulkhead.

B. Vehicle Telescoping Control

Orbital flight forces involved in deployment of the vehicle would be small, consisting of friction only. For ground testing, however, gravity produces substantial resisting forces. A problem is presented by the tendency of the vehicle to tilt during deployment, thus producing a bending moment on the vehicle. To cope with this bending moment, deployment control devices are used consisting of a guide-shoe-and-track assembly and a rub strip (Fig. 13). The bending moment is reacted by a force couple acting at the shoe and rub strip as shown in Fig. 13. The distance between these two forces decreases as the vehicle extends. At full deployment these forces are only three inches apart. Therefore, a small amount of tilt can produce fairly high loads at these points. Due to these anticipated high loads a total of eight guide rails were designed into the vehicle configuration. Subsequent testing, however, proved that the guide rails were over-designed and four rails would be sufficient. It is probable that no guides would be required for deployment in a gravity-gree field, but this is difficult to prove. In any event ground testing requirements will undoubtedly govern the design, and some guide rails will be provided.

Torsional resistance is provided by the guide shoes in the tracks. Any two opposite shoes acting to produce a couple will resist the minute torsional loads.

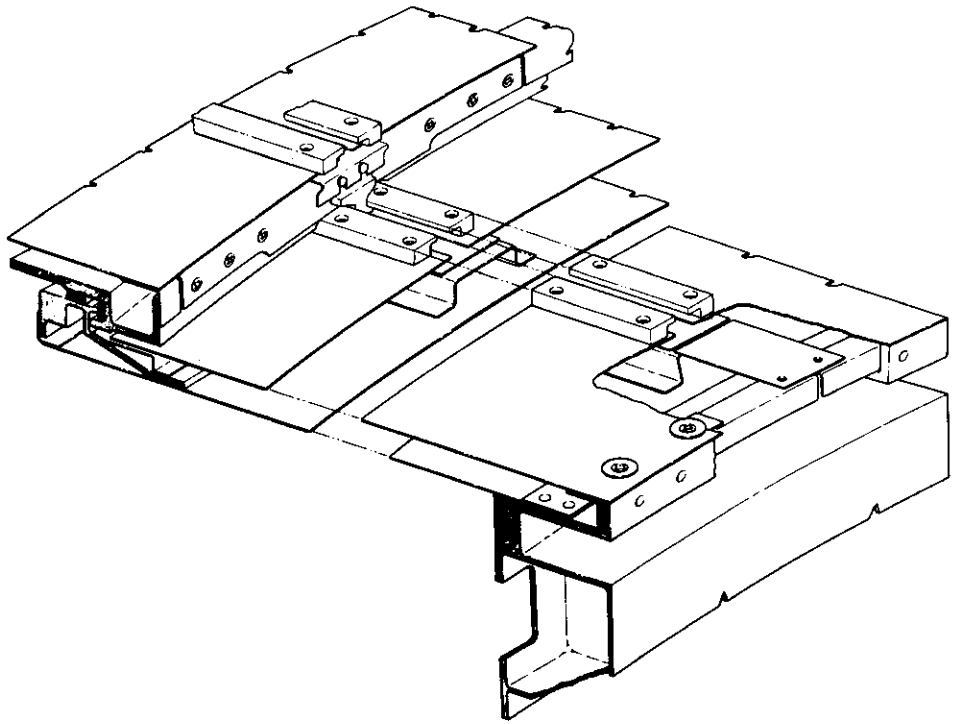

Fig. 11 Structural Configuration Expandable Space Structure Vehicle

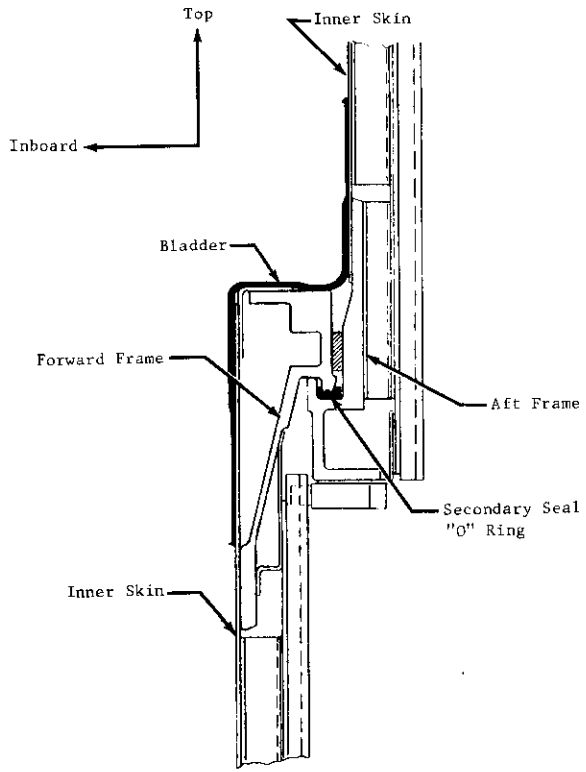

Fig. 12 Expandable Space Structure Machined Mating Frames

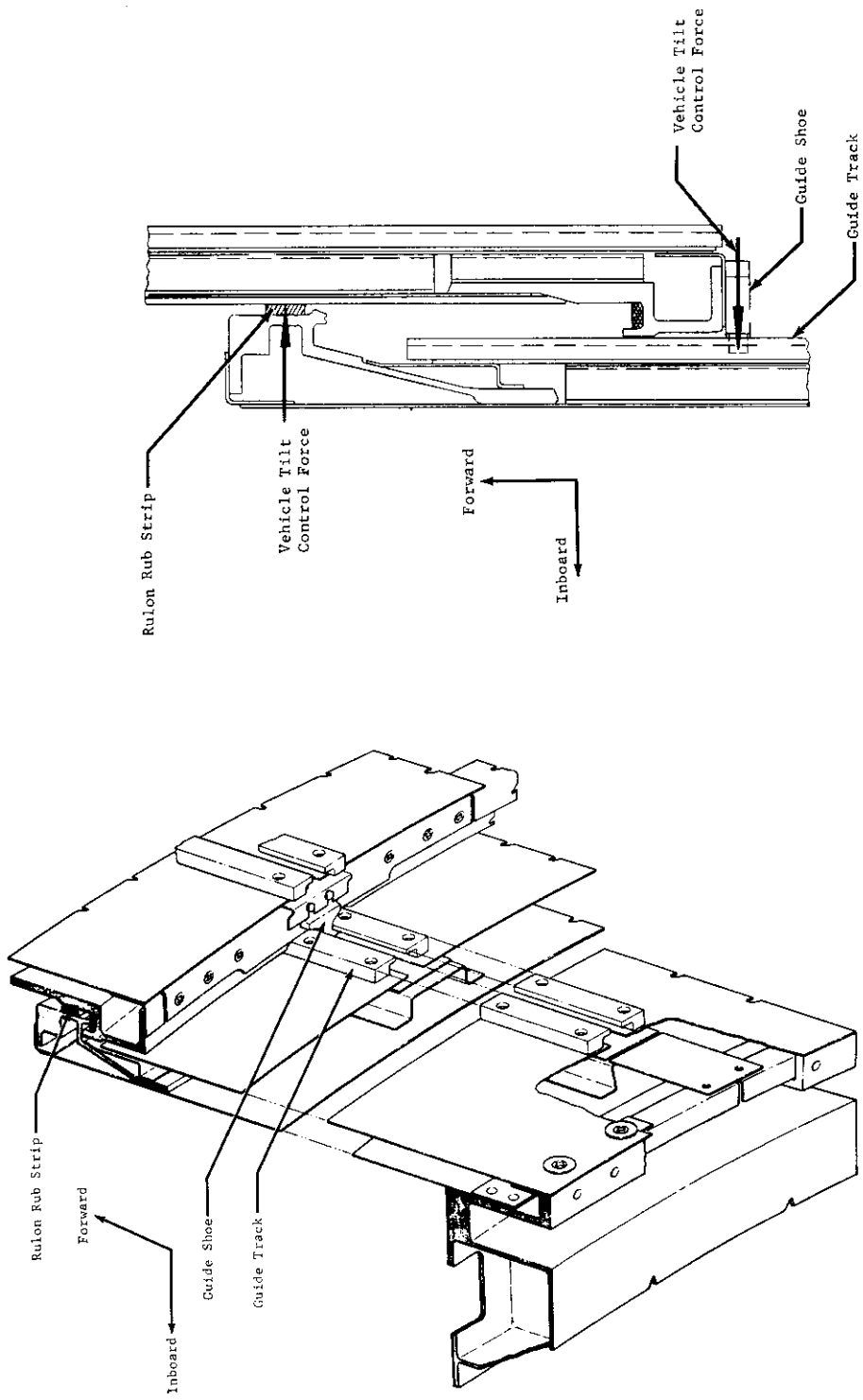

Fig. 13 Tilt Control Moment Reactions

The vehicle is designed to be deployed in orbit and in ground test by admitting low pressure air into the vehicle. A primary seal provides for pressure retention during the deployment. A secondary seal does not function until full deployment is reached.

C. Vehicle Pressurization Control

Two methods of pressure retention are included in the vehicle design. A bladder of Dacron fabric coated on both sides with Hycar rubber provides the primary pressure seal. This consists of an 0.040-in. thick cylindrical sleeve extending the full length of telescoping sections and incorporates a thickened integral "O" ring at each end. The "O" rings are clamped by a retaining ring at each end to hold the bag in place and provide the necessary pressure seal. The bladder is also fastened at the top of each telescoping section by tabs. Rubber bungee cords are also incorporated in the bladder design for testing requirements where the vehicle must be retracted. They physically pull the bladder away from the vehicle walls during retraction and force the bladder to fold compactly. Pictures of the bladder installed in the vehicle are shown in Fig. 14 and 15.

The second method of vehicle pressure retention is provided by a secondary sealing system consisting of the basic vehicle structure plus flattened "O" ring seals at the ends of the telescoping sections. The riveted structure is sealed with sealant between all faying surfaces, and rivets are dipped in sealant prior to driving. The "O" rings consist of a semi-rectangular cross-section shape of neoprene rubber cemented in place in a seal groove as shown in Fig. 12. The two interlocking frames slide together and engage during vehicle deployment, forcing a lip on one frame to compress the seal and prevent leakage (Fig. 12). A second lip, adjacent to the first, bottoms out to carry the structural load to prevent excessive seal compression.

D. Meteoroid Puncture Control

Meteoroid protection is provided by a double-wall structure. A 0.040-gage inner structural skin and a 0.020-gage outer meteoroid bumper, both of 2024 T3 aluminum, are spaced 0.75-in. apart for the desired meteoroid protection.

For 30 days in orbit, and a total length times diameter of 113 sq. ft., the probability of no puncture for this structure is .98 as shown in Fig. 16.

MATERIALS EVALUATION

A test program was initiated to test candidate construction materials for fabrication of the expandable space structure (ESS) vehicle. Testing performed under this program included:

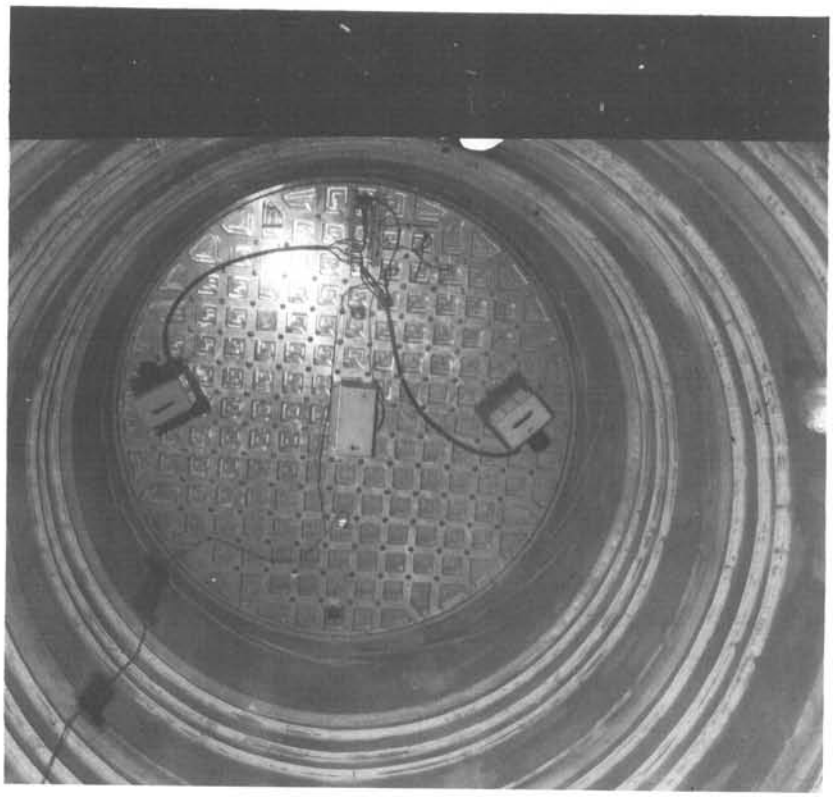

Fig. 14 Internal View, Retracted Position

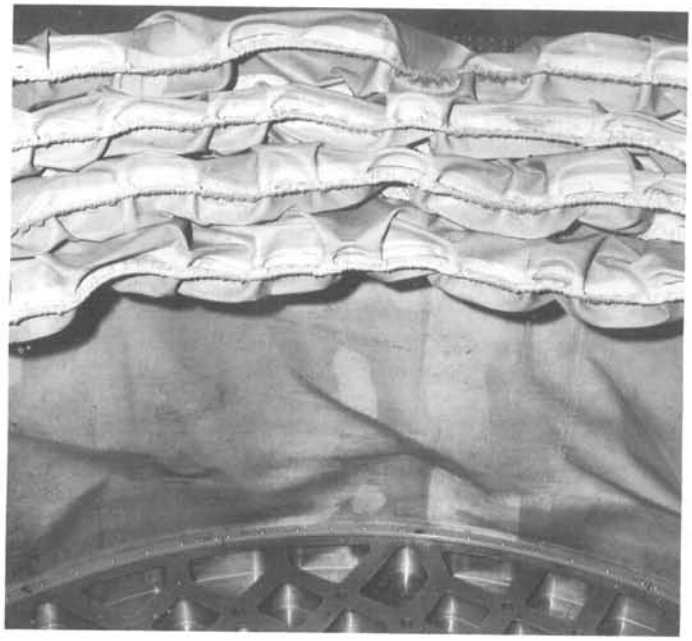

Fig. 15 Internal View, Extended Position

1) Short-term materials outgassing tests;

2) Thermal coatings evaluation tests;

3) Self-sealing bladder materials testing;

4) Long-term space environment materials testing.

The short-term outgassing tests were performed to determine the problems created by outgassing of polymeric materials as it pertained to space environmental testing of the ESS vehicle. The purpose of thermal coating tests was two-fold. Thermal characteristics were determined for vehicle thermal control analyses, and materials degradation tests determined the changes in properties as a result of space environment exposure. Typical outgassing rates are shown in Fig. 17.

Self-sealing bladder materials testing was performed to determine feasibility of self-sealing bladders and not particularly in support of the ESS vehicle design. Results are shown in Table 1.

Material Test Code Number	Puncture Hole Diameter (in.)				
	0.010	0.013	0.020	0.050	0.080
JB-600	0	0	0.007	0.0122	0.085
JB-601	0	0	0	0.0061	0.025
5	0	0	0	0	0.034
6	0	0	0.003	0.006	0.370
Leakage rate is in ml/sec.					

TABLE 1

Long-term materials testing exposed polymeric materials to hard vacuum for periods up to one year and evaluated material properties changes at intervals during this period. Typical results for gasket materials after one year exposure are summarized in Table 2.

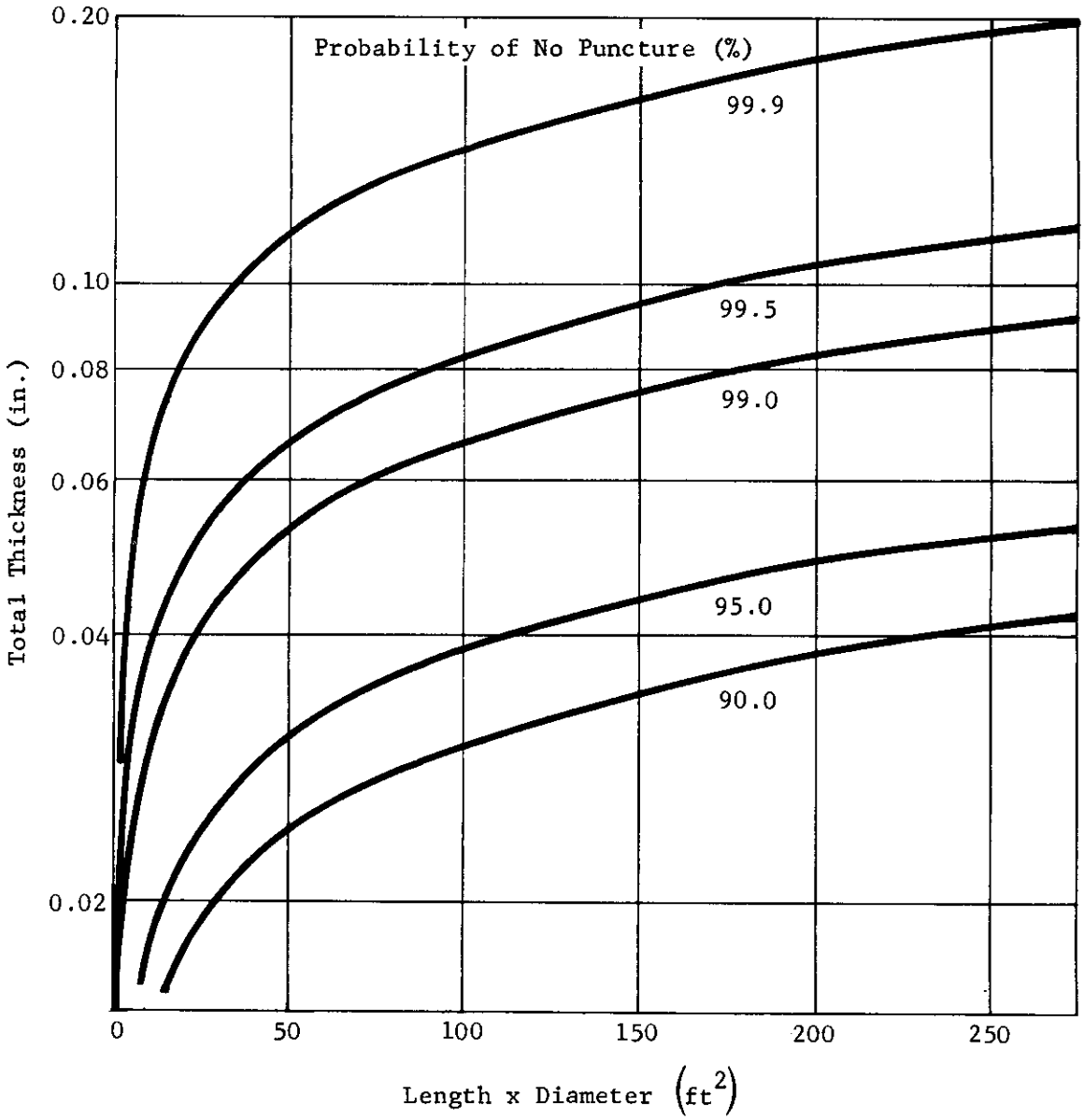

Fig. 16 Effect of Acceptable Probability of No Punctures on the Total Thickness of Aluminum Double-Walled Shell Required for Protection from Meteorites for 30 Days

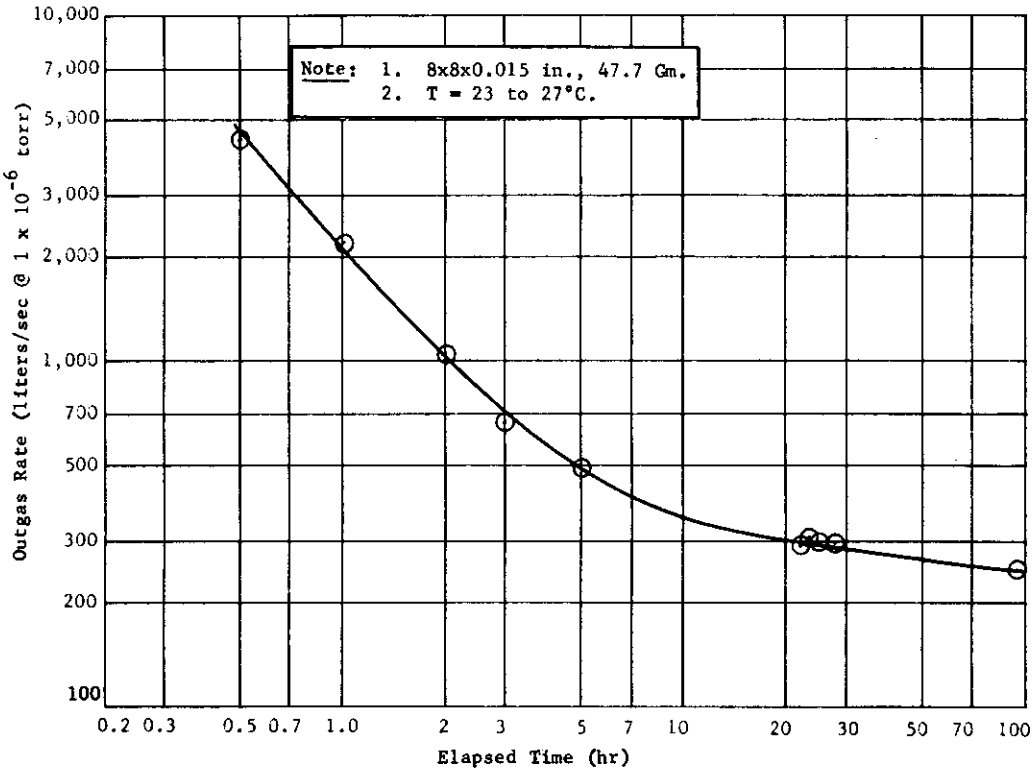

Fig. 17 Outgas Rate vs Time for BF Goodrich 139 KP-509

Table 2 Test Results of Elastomers (Gasket Materials)

Materials Condition	EX-2095 (Neoprene)	Percentage Change	Royalene 200 (Ethylene Propylene)	Percentage Change	C-602-2 (Neoprene)	Percentage Change	121-KP-55 (Neoprene)	Percentage Change	139-KP-9 (Hycar)	Percentage Change
As-Received (Controls)										
Ultimate Tensile Strength (psi)	1762		2780		1925		1671		1961	
Ultimate Percentage Elongation (%)	502		425		208		363		581	
Tensile Stress, 300% E (psi)	921		1813		-		1590		1066	
Shore A Hardness (pts)	56		66		70		69		54	
Compression Set (%)	48		55		14		59		25	
Heat-Aged (100 hr at 158°F)										
Ultimate Tensile Strength (psi)	1800	+2	2180	-22	2225	+16	1776	+6	2116	+8
Ultimate Percentage Elongation (%)	468	-7	350	-17	200	-4	466	+1	550	+6
Tensile Stress, 300% E (psi)	1320	+22	1787	-1			1705	+7	1233	+16
Shore A Hardness (pts)	55	-2	66	0	68	-3	73	+4	57	0
Compression Set (%)	39	-19			11	-29	52	-12	12	-52
Weight Change (%)	-0.8		-0.4		+0.3		-0.3		0	
Hard-Vacuum Exposure (3 mo, $2x10^{-6}$ torr)										
Ultimate Tensile Strength (psi)	1601	-9	2060	-26	2000	+4	1609	-4	2116	+8
Ultimate Percentage Elongation (%)	442	-12	543	+28	183	-12	373	+3	492	-16
Tensile Stress, 300% E (psi)	1116	+22	1920	+6	-		1567	-3	1333	+25
Shore A Hardness (pts)	55	-2	70	+6	75	+7	71	+3	55	+2
Compression Set (%)	35	-27	39	-29	21	+50	50	-15	17	-31
Weight Change (%)	0		-22		+3.2		-1.6		+5.0	
Hard-Vacuum Exposure (6 mo, $1x10^{-5}$ torr)										
Ultimate Tensile Strength (psi)	1820	+3	2800	+70	1893	-	1852	+11.0	2044	+4.8
Ultimate Percentage Elongation (%)	433	-14	383	+10	192	-	500	+38	350	-40
Tensile Stress, 300% E (psi)	1287	+40	2087	+13	-		1323	-17	1987	+86
Shore A Hardness (pts)	55	-2	70	+6	75	+7	70	+3	57	+3
Compression Set (%)	14	-71	15	-73	8	-43	19	-68	5	-80
Weight Change (%)				Data Available at Later Date						
Hard-Vacuum Exposure (12 mo, $1x10^{-5}$ torr)										
Ultimate Tensile Strength (psi)	1820	+6	2717	-2	2125	+10	1747	+5	2161	+9
Ultimate Percentage Elongation (%)	467	+7	467	+10	196	-6	358	-1	508	-13
Tensile Stress, 300% E (psi)	1162	+26	1811	-1	-		1671	+5	1609	+32
Shore A Hardness (pts)	57	+2	65	-2	74	+6	69	0	60	+11
Compression Set (%)	13.2	-73	13.0	-76	10.0	-29	23.8	-38	6.8	-72

TESTING

Testing of the completed expandable space structure (ESS) vehicle was accomplished under Phase III of the program. The tests performed are as follows:

A. Proof Pressure Test

This test was performed to prepare the vehicle for subsequent activities with the vehicle pressurized. The internal bladder was deleted, and the pressure was retained by the secondary "O" ring seals on each telescoping section. The vehicle was subjected to proof pressure, and it sustained this pressure with no evidence of structural malfunction. The proof pressure was 12.1 psi, which is 10% over the design limit pressure of 11 psi.

B. Functional Test, Pressure-Actuated Deployment

The purpose of this test is to demonstrate expansion of the ESS vehicle using internal air pressure for deployment.

The first pressure-actuated deployment test was performed with the bladder installed unlubricated and required .7 psi to extend the vehicle to full length. To evaluate the effects of friction on deployment, the bladder was removed from the vehicle and lubricated with Dow Corning high vacuum grease. A cloth was lightly dampened with the grease and rubbed on the outside surface of the bladder. Only enough grease to leave an invisible film was used. The same thin coating was applied to the inside of the aluminum skin in contact with the bladder. The bladder was then reinstalled in the ESS vehicle. Subsequent testing of the vehicle showed the deployment pressure to be 0.25 psi. Figure 14 shows the folded bladder in the retracted position. Figure 15 shows the bladder with vehicle in the extended and pressurized condition. Note the three bungee cords per section that assist in bladder folding during retraction.

C. Combined Seal Leak Test

Two tests of the combined seals were performed in an atmospheric environment. For this test, the vehicle was placed in a temperature-stabilized room and pressurized to 11.25 psi. The vehicle pressure was adjusted again to 11.25 psi pressure after the internal temperature had stabilized at room temperature. The valves were then sealed shut and the pressurized vehicle allowed to stand for 54 hr. At the end of this period, the pressure had dropped only 0.05 psi, a leakage rate of 0.001 psi/hr. This amounts to a loss of 0.045 cu. ft./hr. of air at standard conditions, or 0.0034 lb./hr.

D. Secondary Seal Leak Test

This test was accomplished immediately after the combined seal leak test, and without removing the bladder from the vehicle. The bladder was unsealed and unfastened at the bottom end and tied back to admit internal air pressure between the bladder and the vehicle structure.

For this test, the vehicle was pressurized to 11.0 psi and allowed to stand for a period of 7 hr. The pressure during this period decayed approximately 0.7 psi, leakage rate of 0.1 psi/hr. This leakage rate is adequate to permit an astronaut to locate and make repairs to the primary pressure seal without losing an excessive amount of vehicle pressure.

E. Environmental Chamber Test

Environmental chamber testing of the ESS vehicle was performed by Lockheed Missiles and Space Company in its high vacuum orbital simulator (HIVOS) test chamber. For this test, the necessary instrumentation was installed at Martin-Denver, and the ESS vehicle was shipped to Lockheed at Sunnyvale, California.

1. Heat Flux Simulator

A solar heating simulator was designed and fabricated by Lockheed. General Electric 1600 T3 infrared heat lamps were installed on the simulator in vertical rows to provide simulated solar, earth emitted, and earth reflected heating to the vehicle.

2. HIVOS Testing

Deployment Test - The ESS was mounted on the door of the HIVOS environmental chamber and the heat flux simulator lowered over it and fastened in place. The door, which is the bottom of the chamber, was raised with the ESS in place, and closed. The HIVOS was pumped down to a pressure level of 3×10^{-6} torr. After 2 hr. in this vacuum, vehicle deployment was started. Deployment motion was monitored by TV. The cannistered TV camera is seen in Fig. 18. For this testing, the camera was pointed upward. Deployment was smooth with a slight tilting and subsequent straightening action near the end of travel of each section. The maximum pressure during deployment was 0.28 psi to full extension. This compares with a pressure of 0.25 psi for deployment in the atmosphere.

Leakage Test - Leakage tests were made using the 0 to 15 psi absolute pressure gage transducer within the vehicle. Compensating for temperature changes, the pressure in the ESS dropped from 10.95 to 10.90 psi in 8 hr., a loss of 0.00625 psi/hr., or 0.03 cu. ft./hr. of gas (at standard conditions). This leakage rate is approximately six times as great as that measured in the atmosphere but is probably not as accurate. This number may be somewhat in error because of the short test duration and temperature fluctuations.

Thermal Test - The space thermal environment was simulated during this test. Only the cylindrical portions of the vehicle were under test. The top and bottom were thermally isolated by a multilayer radiative type super-insulation covering these areas.

The vehicle test configuration had multilayer insulation installed between the inner and outer skins. The outer skin had been previously painted with Dow Corning Q-9-0090 (white) dimethyl silicone paint. The heat flux was provided by the heat flux simulator cage shown in Fig. 18, which had previously

been placed over the ESS vehicle. The solar, earth-emitted, and earth-reflected heat was simulated by vertical rows of 3/8 in. diameter by 18 in. long tungsten quartz heat lamps. These are General Electric 1600 T3 infrared lamps seen in Fig. 18.

During the thermal test, the HIVOS chamber remained evacuated and the chamber walls were cooled to liquid nitrogen temperatures to simulate outer space. The heat lamps were turned on, with the voltage in each vertical lamp row controlled to give the proper heat flux in that area. The actual heat flux that the vehicle would see in flight is shown in Fig. 19. Note that the absorptance (α) of the vehicle coating is 0.16 for the solar radiation spectrum and 0.90 for the long wavelength of the earth-emitted radiation. The actual heat flux values used for tests are shown in Fig. 20. These values compensate for a quoted absorptance (α) of 0.20 for the thermal coating in the heat lamp infrared spectrum in place of the solar absorptance of 0.16.

To simulate this heat flux curve, the heat lamp voltage varied from 44 volts to a maximum of 135 and then down to 50 around the periphery of the ESS vehicle producing the proper input heat distribution.

The raw data from the thermal test instrumentation was reduced and corrected for the following factors:

a. Variation in coating properties;

b. Variation of absorptance with infrared wave lengths;

c. Unpainted guide rails;

d. Internal blower temperature.

The temperatures from this analysis are shown in Fig. 21 and show fair correlation with test results for outer skin temperatures, shown in Fig. 22. Although there is not exact agreement between test temperature data and computed values, the agreement is satisfactory and indicates that the original computed values of temperature for the vehicle in earth orbit flight are applicable.

F. Cycle Test, Ground Environment

The cycle test was to demonstrate reliability and repeatability of deployment of the ESS vehicle in an atmospheric environment. The test plans called for 20 cycles of extension and retraction. Many unplanned extensions, retractions, and pressurization cycles were performed before the formal cycle test. Consequently, it was decided that the full 20 cycles would not be performed during this test. The vehicle now has accomplished over 30 tabulated cycles, including those performed in the cycle test.

G. Structural Tests

The structural confirmation of the ESS vehicle consisted of two tests, a boost phase load test and an ultimate pressure test.

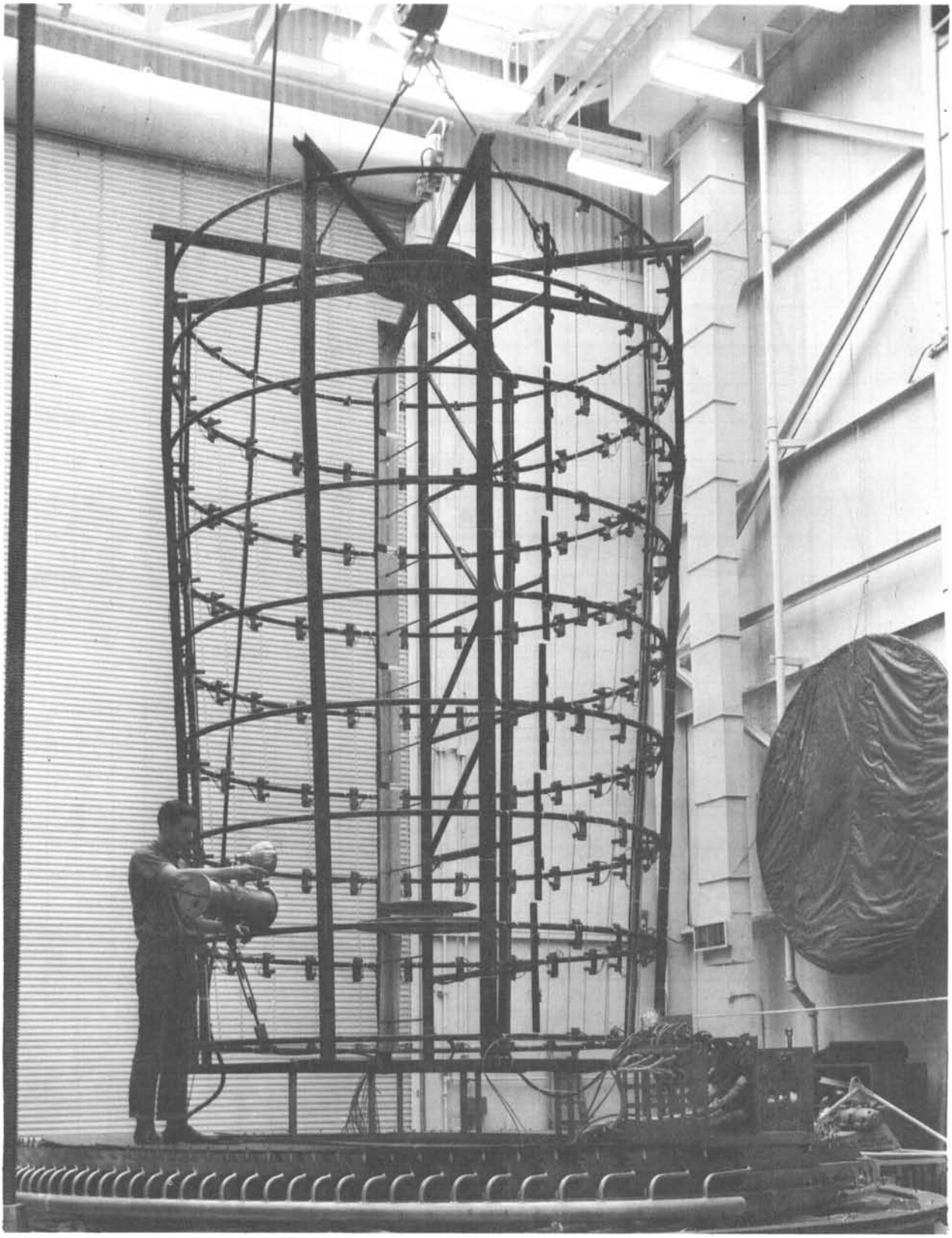

Fig. 18 Heat Flux Simulator Cage

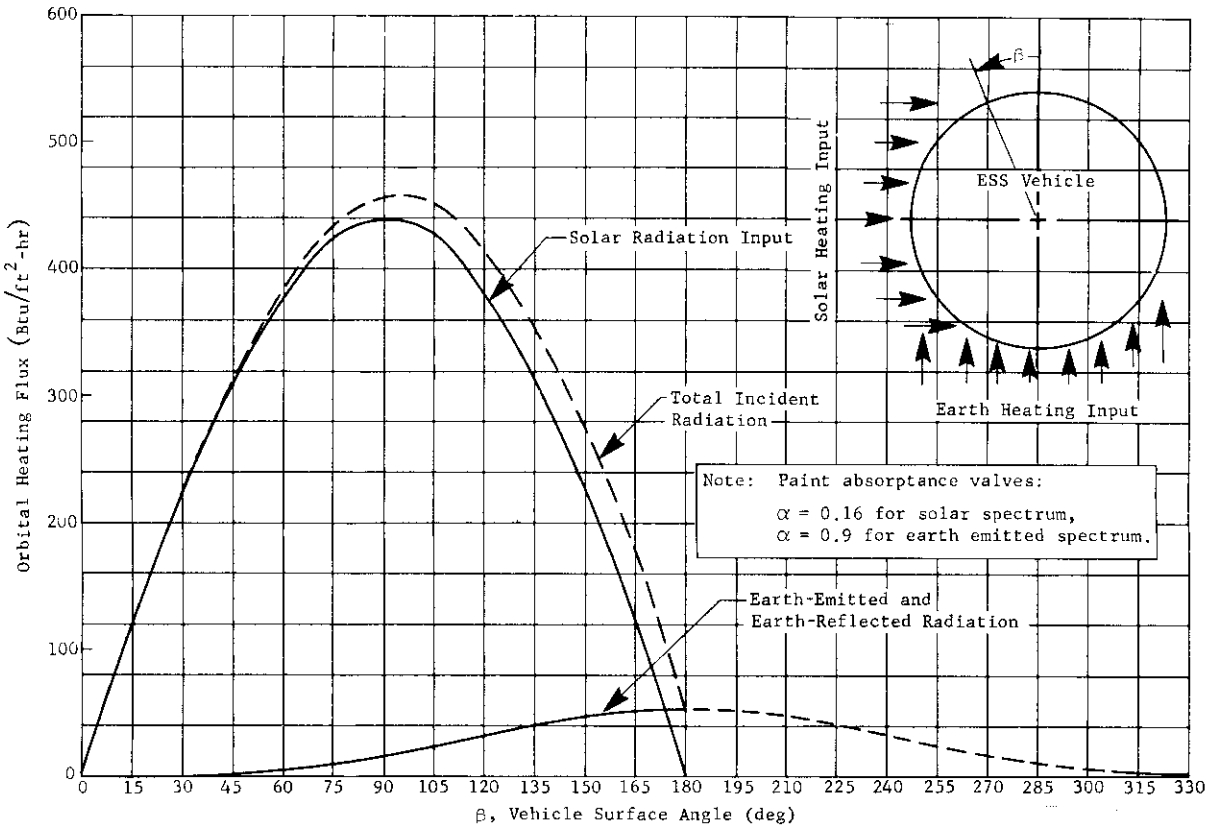

Fig. 19 Space Flight Heat Flux (Polar Orbit)

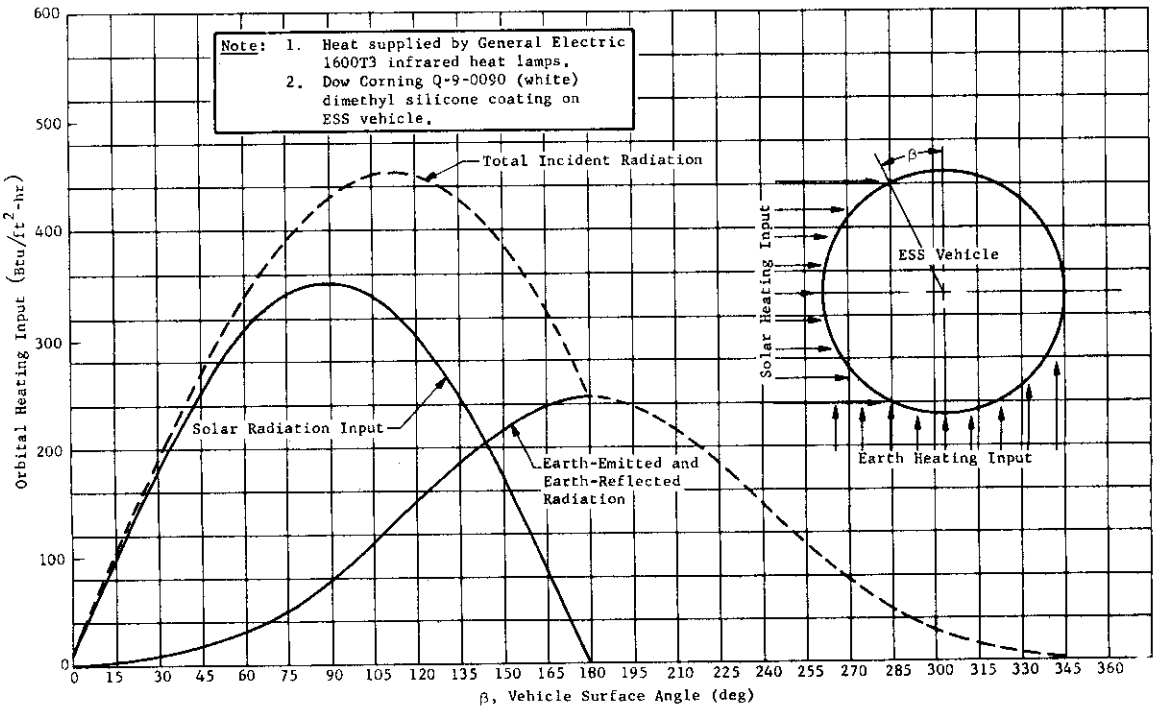

Fig. 20 Heat Flux Input for Thermal Test

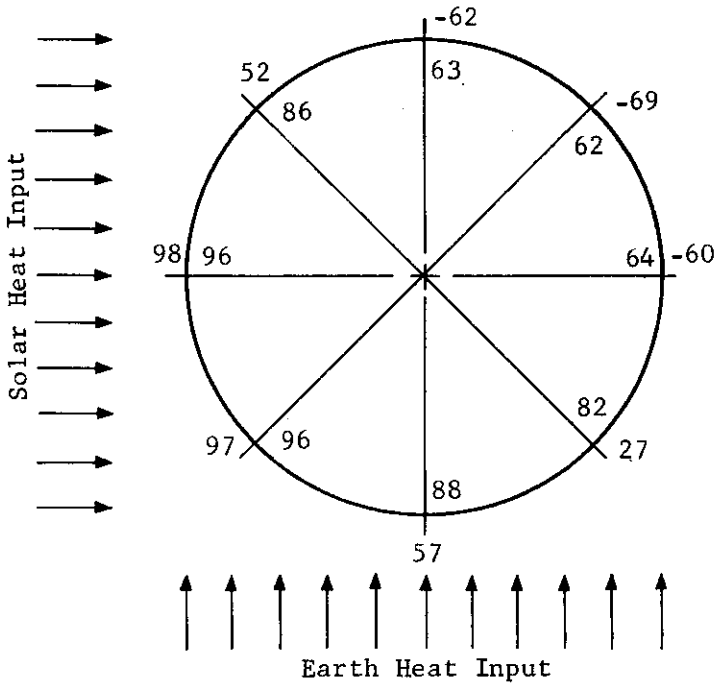

Fig. 21 Caluclated Temperatures using Revised Input Data

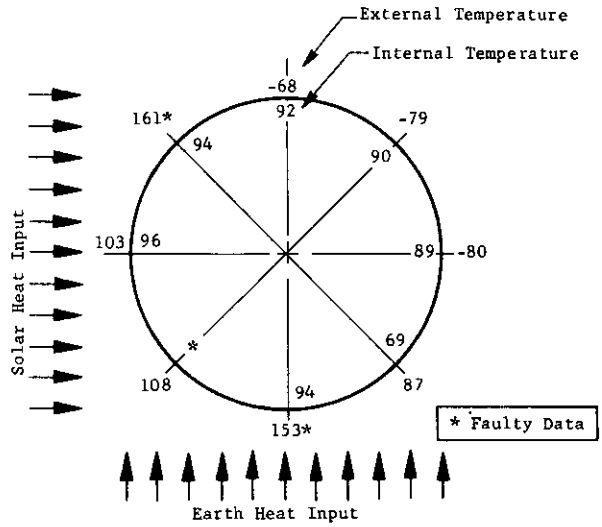

Fig. 22 Thermal Test Recorded Temperatures (°F)

1. Boost Phase Load Test

The objective of this test was to demonstrate the capability of the expandable space structure to withstand maximum loads imposed during boost. The critical loading condition occurs during maximum dynamic pressure when critical shear, moment, and compressive loads are imposed on the outer section with the vehicle in the collapsed position. At the same time, burst and collapse pressures are imposed on the outer skin panels.

The vehicle was mounted to a base loading fixture in the collapsed position, and the outer section was bolted down. All applied loads were reacted in the base fixture. The vehicle was filled with water to minimize the hazard. It was then pressurized at the crown of the dome to 5.8 psig. Axial and side loads were applied through a loading head attached to the forward adapter skirt. Side load was also applied directly into the skirt. Burst pressure load was simulated on the leeward stringers by applying load directly through load beams. Collapse pressure was simulated on the wind-ward external skin panel with pressurized air bags.

2. Ultimate Pressure Test

The objective of the ultimate pressure test was to demonstrate capability of the space station structure to withstand 150% operating pressure (16.5 psig) internally without failure. The vehicle was complete including internal bladder.

During the ultimate pressure test the vehicle retained pressure with no apparent leakage, although a precise leakage test was not performed in conjunction with this test. A routine check of the vehicle after the ultimate pressure test showed no evidence of structural failure. This was to be expected since most of the pressure structure was designed to criteria other than strength requirements.

POTENTIAL USES

Potential uses of ESS vehicles are shown in Fig. 23 through 27. Figure 23 shows the ESS used in artificial gravity simulation vehicles. In this concept two space capsules are joined together by a telescoping tube. The whole unit is retracted for launch and the telescoping tube is expanded in orbit to provide a rigid joining structure for the two end capsules. The tube would provide the necessary structure for centrifugal loads (artificial gravity) produced by spinning and provide a meteoroid protection passageway between capsules for personnel traffic. The tube could be pressurized to provide a shirt-sleeve environment if desired. Advantages of this approach over a cable system joining the two end capsules include bending and torsional rigidity. This eliminates the boat-rocking sensation in the end capsule due to personnel movement and the torsional windup which results with a cable system. In addition, cable tangling during deployment is eliminated as a potential hazard.

Figure 24 shows a space station using an expandable space structure tube to provide physical separation of the personnel capsule on one end and a nuclear power package on the other end.

Figure 25 shows a manned space vehicle using the telescoping structure as a partial garage for a personnel re-entry vehicle. Such a garage could provide a pressurized shirt-sleeve environment around the vehicle for making repairs, inspections, etc., and would prevent loss of tools in space. The garage could be large enough to accept the entire re-entry vehicle and have a closure door if desired.

Figure 26 shows a space vehicle with a portion of the vehicle designed of an expandable space structure. This vehicle illustrates a concept that could be used to circumvent boost-imposed payload length limitations.

Figure 27 shows the entire vehicle fabricated as an expandable space structure.

CONCLUSIONS AND RECOMMENDATIONS

The expandable space structure program has been successfully completed. In retrospect, the following observations can be made concerning expandable structure:

- Large size telescoping structure fabricated of individual rigid segments is quite feasible.
- Short coupling of rigid cylinders (small engaged length/diameter) at full extension does not necessarily produce binding if properly designed.
- Telescoping structure is somewhat heavier than nontelescoping structure, but not prohibitively so.
- Deployment of semirigid telescoping structure by internal pressure is feasible and is an acceptable means of extension.
- Leakage rates of telescoping structure can be kept low enough that long-term internal pressurization is feasible and practical.

The weight of the present ESS vehicle is approximately 40% heavier than that of a comparable nontelescoping structure. The majority of this weight difference is due to the large eccentricity in longitudinal load in the inner skins in stepping down from one telescoping segment to the next. The ring frames are heavy to react this resulting moment. The large eccentricity is due in turn to the double-wall structure for meteoroid protection. If the outer skins were designed to package against the inner skin in the retracted vehicle position and be spring loaded to move away from the inner skin after vehicle extension, the eccentricity can be reduced and a considerable weight savings achieved. The telescoping structure weight would then be much closer

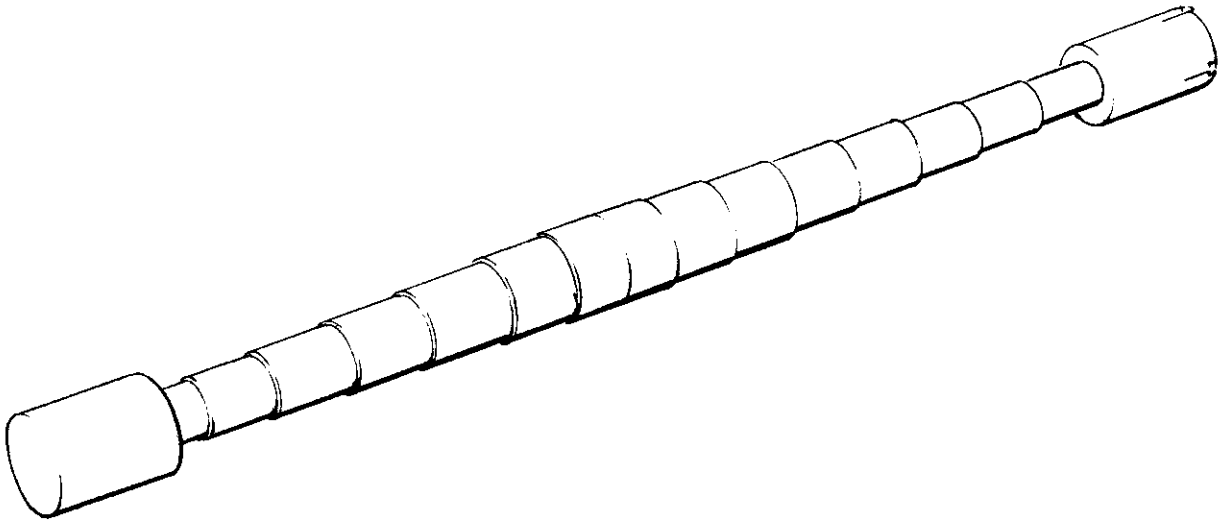

Fig. 23 Artificial Gravity Simulation Space Vehicle using Expandable Space Structure

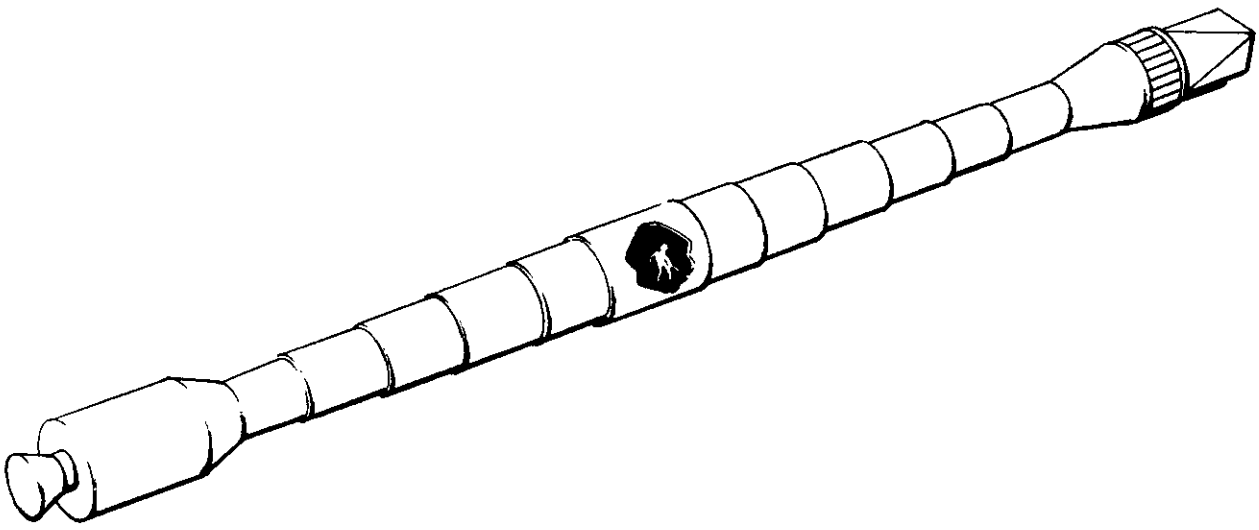

Fig. 24 Space Station Manned Module Separated from Nuclear Power Supply by Expandable Space Structure

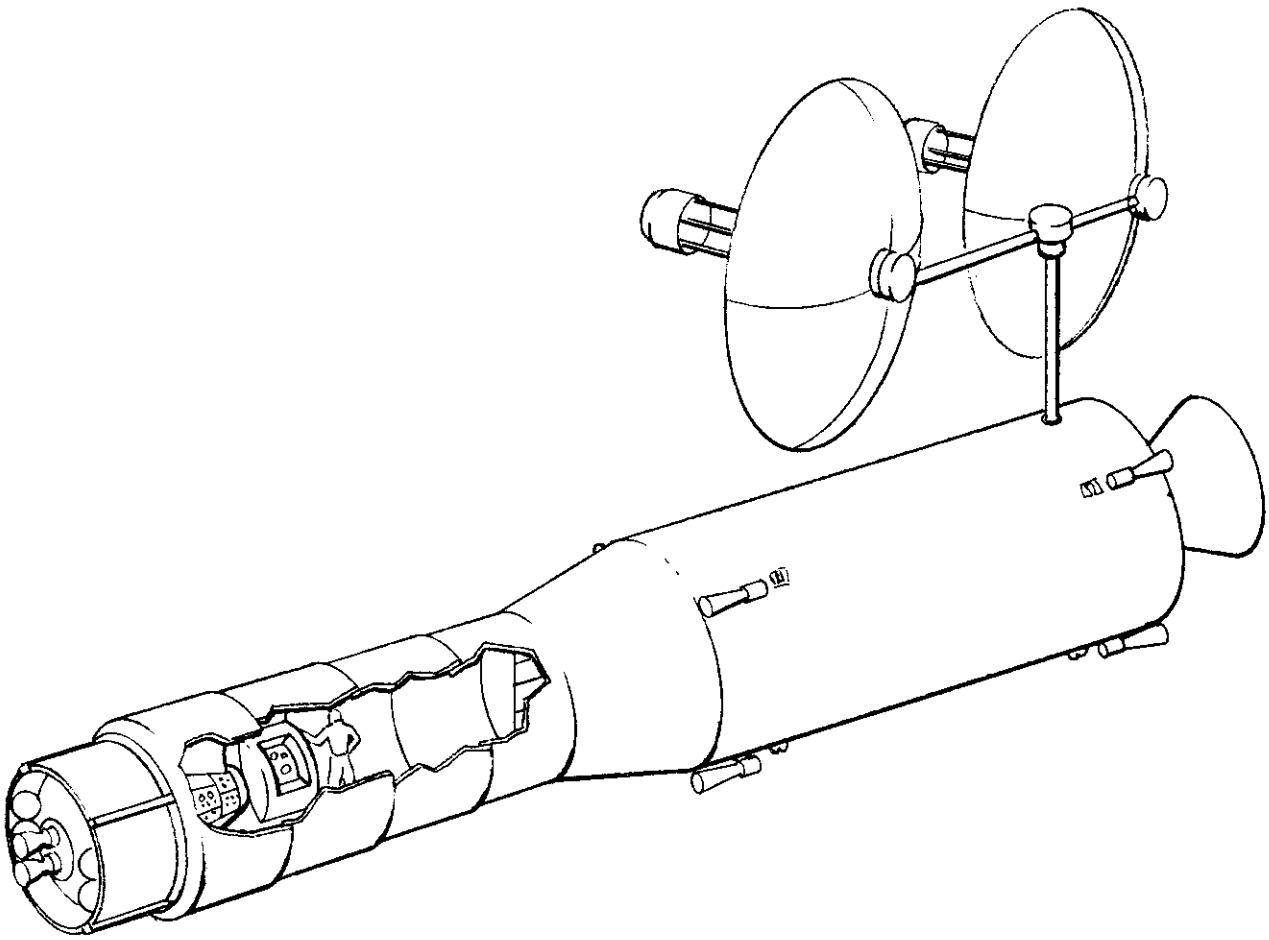

Fig. 25 Expandable Space Structure used as Partial Garage for Re-Entry Vehicles

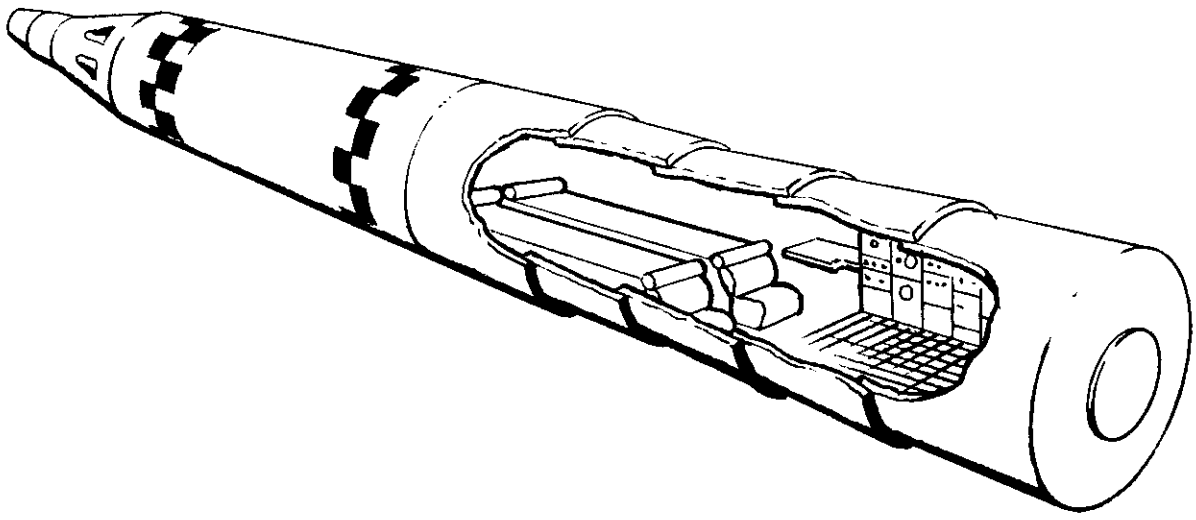

Fig. 26 Space Vehicle using Partial Construction of Expandable Space Structure for Living Quarters

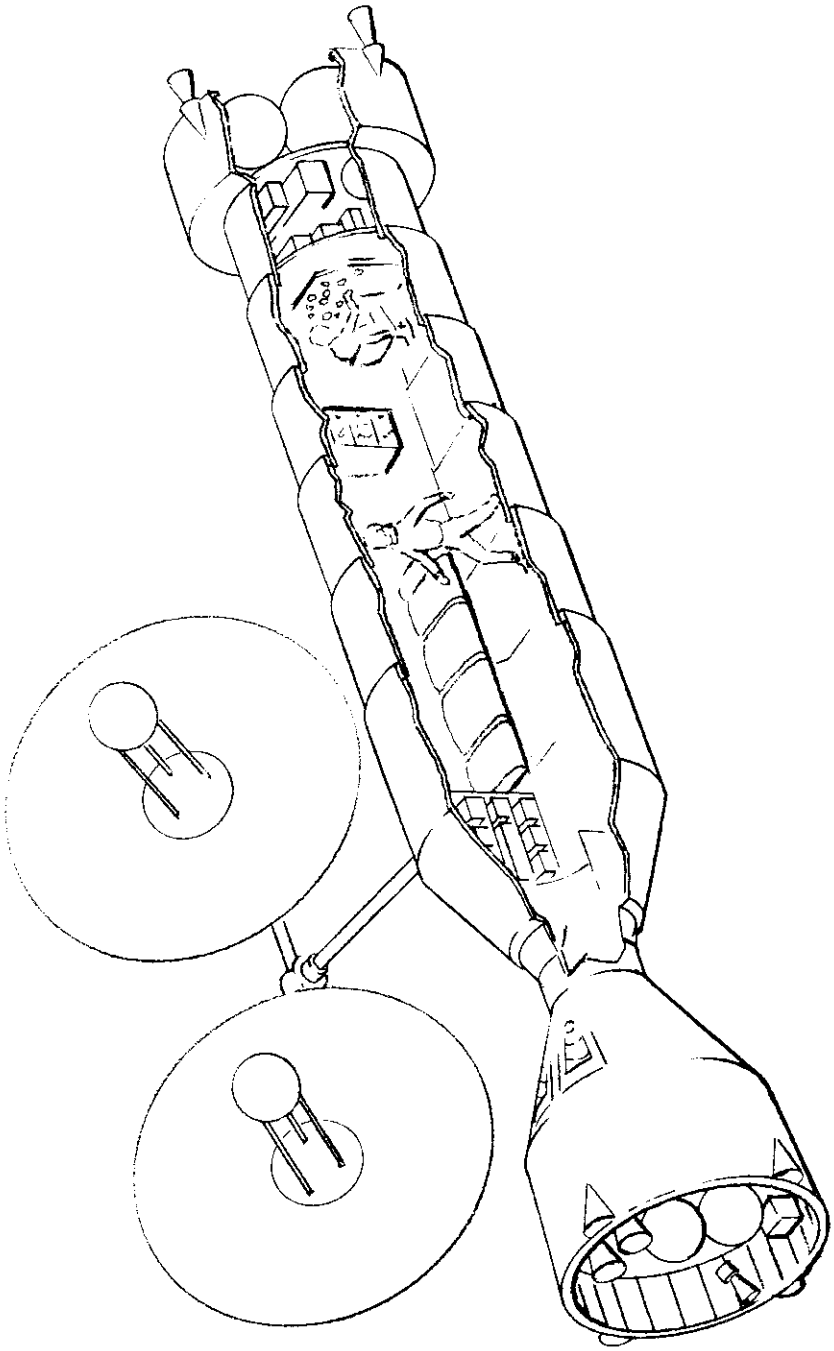

Fig. 27 Space Vehicle Designed Entirely of Expandable Space Structure shown Rendezvoused with Re-Entry Vehicle

to that of a nontelescoping structure and possibly equal it. An advantage of the telescoping structure is that most of the outer skin can be light. It does not have to be heavy gage to resist aerodynamic heating and panel flutter.

It is recommended that telescoping expandable space structure be seriously considered for the following applications:

1. Structural applications for manned or unmanned space vehicles where vehicle length proves to be restricted by booster considerations or other problems;

2. Structural applications for joining multiple space units, such as joining two or more space capsules in an artificial gravity configuration. The tubular telescoping components provide a structure that is rigid in bending, in torsion, and axially, once extended. It provides protected passageway for personnel moving from one vehicle to another;

3. Space vehicles, either manned or unmanned, where a large amount of relatively empty space is desired.

Expandable space structures of the type described in this report can provide a long-term pressurized environment for human occupants and when painted with suitable coatings can provide tolerable occupancy temperatures by passive thermal control. This is desirable for passageway, etc., as well as for basic space vehicle modules.